Arabian Journal of Chemistry (2015) **8**, 632–643

King Saud University

Arabian Journal of Chemistry

www.ksu.edu.sa
www.sciencedirect.com

ORIGINAL ARTICLE

The effect of noble metals on catalytic methanation reaction over supported Mn/Ni oxide based catalysts

Wan Azelee Wan Abu Bakar *, Rusmidah Ali, Nurul Shafeeqa Mohammad

Department of Chemistry, Faculty of Science, Universiti Teknologi Malaysia, 81310 Skudai, Johor, Malaysia

Received 7 December 2012; accepted 9 June 2013
Available online 17 June 2013

KEYWORDS

Carbon dioxide;
Manganese–nickel oxide;
Noble metal;
Methanation;
Natural gas

Abstract Carbon dioxide (CO_2) in sour natural gas can be removed using green technology via catalytic methanation reaction by converting CO_2 to methane (CH_4) gas. Using waste to wealth concept, production of CH_4 would increase as well as creating environmental friendly approach for the purification of natural gas. In this research, a series of alumina supported manganese–nickel oxide based catalysts doped with noble metals such as ruthenium and palladium were prepared by wetness impregnation method. The prepared catalysts were run catalytic screening process using in-house built micro reactor coupled with Fourier Transform Infra Red (FTIR) spectroscopy to study the percentage CO_2 conversion and CH_4 formation analyzed by GC. Ru/Mn/Ni(5:35:60)/Al_2O_3 calcined at 1000 °C was found to be the potential catalyst which gave 99.74% of CO_2 conversion and 72.36% of CH_4 formation at 400 °C reaction temperature. XRD diffractogram illustrated that the supported catalyst was in polycrystalline with some amorphous state at 1000 °C calcination temperature with the presence of NiO as active site. According to FESEM micrographs, both fresh and used catalysts displayed spherical shape with small particle sizes in agglomerated and aggregated mixture. Nitrogen Adsorption analysis revealed that both catalysts were in mesoporous structures with BET surface area in the range of 46–60 m^2/g. All the impurities have been removed at 1000 °C calcination temperature as presented by FTIR, TGA–DTA and EDX data.

1. Introduction

To date, methanation reaction has been widely used as a method of removal carbon dioxide from gas mixtures in hydrogen or ammonia plants, for purification of hydrogen stream in refineries and ethylene plants. Nickel is a well established catalyst decades ago since they are known to be active in hydrogenation, dehydrogenation, hydrotreating and steam reforming reaction and thus have gained great attention (Richardson, 1982 and Azadi et al., 2001). Nickel oxide has

* Corresponding author. Tel.: +60 13 7466213.
E-mail addresses: wazelee@kimia.fs.utm.my, wanazelee@yahoo.com (W.A. Wan Abu Bakar).

Peer review under responsibility of King Saud University.

Production and hosting by Elsevier

1878-5352 © 2013 Production and hosting by Elsevier B.V. on behalf of King Saud University.
http://dx.doi.org/10.1016/j.arabjc.2013.06.009

been widely used due to high activity and low cost (Mok et al., 2010). However, most nickel-based catalysts undergo deactivation due to sintering and carbon deposition during reaction. Thus, nickel based catalysts are needed to be modified in order to produce a catalyst resistant towards deactivation. Combination of nickel catalyst with other transition metal oxides and other promoters has been reported to be active in many reactions such as catalytic oxidation and steam reforming. Addition of manganese oxides are effective in decreasing the coke formation in the dry reforming of methane over Ni/Al_2O_3 (Park et al., 2010 and Ouaguenouni et al., 2009). Although noble metals such as Ru, Rh, Pd and Pt, are known to give high activity and selectivity, but because of limited availability and high cost of them have restricted their applications. In this work, we modified the nickel oxide based catalyst by incorporating manganese and noble metals into the system throughout the impregnation method and applied them in catalytic methanation reaction. Then, the potential catalyst was characterized using different techniques and tested in the flow of CO_2 and H_2.

2. Experimental

2.1. Preparation of catalysts

Impregnation method was used in the production of all catalysts according to the previous work (Wan Abu Bakar et al., 2010). 5 g $Ni(NO_3)_2{\cdot}6H_2O$ purchased from GCE Laboratory Lab was dissolved in little amount of distilled water. Mixed solution was prepared by mixing appropriate amount of $MnCl_2{\cdot}2H_2O$ and noble metal salts ($Pd(NO_3)_2{\cdot}xH_2O$ and $RuCl_3{\cdot}xH_2O$) according to the desired ratio (40:60, 20:80, 5:35:60, 5:15:80). The solution was stirred continuously for 20 min. Alumina beads with a diameter of 3 mm were immersed in the solution for 20 min as support material in this study. It was then aged in the oven at 80–90 °C for 24 h. It was then followed by calcination in the furnace at preferred calcination temperatures (400, 700 and 1000 °C) for 5 h using a ramp rate of 5 °C/min in order to remove all the metal precursors, impurities and excessive of water .

2.2. Catalytic performance test

All the prepared catalysts underwent catalytic screening test to study their catalytic activity towards CO_2/H_2 methanation reaction using in house built micro reactor coupled with FTIR Nicolet Avatar 370 DTGS as illustrated in Fig. 1. The analysis was carried out using simulated natural gas comprising of continuous flow of CO_2 and H_2 in 1:4 ratio with the flow rate of 50 cm^3/min. The weight hourly space velocity was fixed at 500 mL g^{-1} h^{-1}.The prepared catalyst was put in the mid of the glass tube with diameter 10 mm and length of 360 mm. Glass wool was used at both ends of the Pyrex glass tube and positioned in the micro reactor furnace for catalytic testing. Heating of the reactor was supplied by a programmable controller which was connected via a thermocouple placed in the centre of the furnace. A mass flow controller was used to adjust the feed of gas flow. The catalytic testing was performed from 80 °C up to the maximum reaction temperature studied (400 °C) with the increment of 5 °C/min. The FTIR spectra were recorded in the range of 4000–450 cm^{-1} with 8 scans at 4 cm^{-1} resolution to maximize the signal to noise (S/N) ratio. Methane formation was detected by Hewlett Packard 6890 Series GC System (Ultra 1) with 25.0 m × 200 μm × 0.11 μm nominal columns, with helium (He) gas as the carrier gas with a flow rate of 20 mL/min at 75 kPa, and Flame Ionization Detector (FID).

2.3. Characterization of catalysts

XRD analysis was conducted using a Siemens D5000 Crystalloflex X-ray Diffractometer equipped with Cu target (λ Cu-Ka = 1.54 Å) radiation between 20° to 80° (2θ) running at 40 kV and 40 A. The morphology of catalysts was visualized using a Field Emission Scanning Electron Microscope (FESEM) coupled with EDX analyzer for semi quantitative composition. The Nitrogen Adsorption analysis was obtained throughout Micromeritics ASAP 2010. Functional group present was detected by Fourier Transform Infra-Red (FTIR). Thermal stability of desired catalyst was carried out by TGA–DTA analysis.

3. Results and discussion

3.1. Catalytic performance on CO_2/H_2 methanation reaction

3.1.1. Catalytic activity screening of alumina supported nickel oxide based calcined at 400 °C for 5 h

The supported monometallic oxide catalyst (Ni/Al_2O_3, Mn/Al_2O_3, Ru/Al_2O_3 and Pd/Al_2O_3) calcined at 400 °C showed very low catalytic activity towards CO_2/H_2 methanation reaction. Ni/Al_2O_3 catalyst gave a high CO_2 conversion of 13.30% at maximum reaction temperature studied compared to the other oxides catalysts (Table 1). These catalysts did not able to achieve high conversion at low reaction temperature however they showed the capability to be used in methanation reaction. Thus by incorporating manganese and noble metals into system, they would enhance the catalytic activity.

Referring to Table 1, it can be observed that the addition of Mn slightly increased the catalytic performance compared to the monometallic oxide (Ni/Al_2O_3) catalyst. At 400 °C reaction temperature, $Mn/Ni(20:80)/Al_2O_3$ catalyst gave 17.50% of CO_2 conversion while $Mn/Ni(40:60)/Al_2O_3$ catalyst was able to obtain 15.30% conversion only. It is probably due to the largest amount of dopant blocking the pores structure of the catalyst and thus decreasing the activity. Besides, the catalytic performance of both $Ru/Ni(20:80)/Al_2O_3$ and $Pd/Ni(20:80)/Al_2O_3$ catalysts also increased in a little amount. As can be noticed in Table 1, these bimetallic oxide catalysts have a low percentage of CO_2 conversion (< 18%). Thus, alumina supported manganese–nickel oxide based catalyst was modified by incorporating with noble metal, ruthenium and palladium to study their effect towards the catalytic activity.

Incorporating palladium (Pd) into this catalyst ($Pd/Mn/Ni(5:35:60)/Al_2O_3$) slightly increased the catalytic performance towards CO_2 conversion up to 25.30%. Meanwhile, when ruthenium ($Ru/Mn/Ni(5:35:60)/Al_2O_3$) was added as a co-dopant further reduction of catalytic performance was observed which only gives 14.00% CO_2 conversion. The decreasing performance of this catalyst could be due to the Ru precursor, $RuCl_3.xH_2O$ used in this research. A small amount of chloride ion present in Ru/Al_2O_3 catalyst could give poisoning effect to

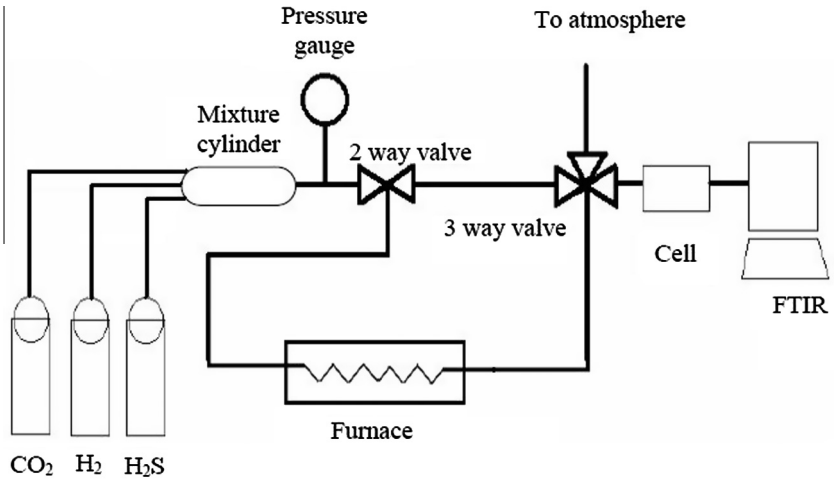

Figure 1 Schematic diagram of home-built micro reactor coupled with FTIR.

Table 1 Percentage CO_2 conversion over alumina supported NiO based catalysts calcined at 400 °C for 5 h.

Catalysts	Reaction temperature (°C)			
	100	200	300	400
	% CO_2 conversion			
Monometallic oxide				
Ni(100)/Al_2O_3	4.60	6.20	9.50	13.30
Mn(100)/Al_2O_3	1.01	1.40	2.08	3.50
Ru(100)/Al_2O_3	1.40	1.62	2.30	4.42
Pd(100)/Al_2O_3	2.10	3.34	4.70	7.50
Bimetallic oxide				
Mn/Ni(40:60)/Al_2O_3	4.70	6.80	10.21	15.30
Mn/Ni(20:80)/Al_2O_3	6.10	8.30	13.40	17.50
Ru/Ni(20:80)/Al_2O_3	2.30	4.90	5.94	7.21
Pd/Ni(20:80)/Al_2O_3	2.80	3.30	6.20	9.10
Trimetallic oxide				
Pd/Mn/Ni(5:35:60)/Al_2O_3	3.50	9.30	16.20	25.30
Ru/Mn/Ni(5:35:60)/Al_2O_3	3.30	5.50	11.00	14.00
Pd/Mn/Ni(5:15:80)/Al_2O_3	5.20	10.40	22.00	49.00
Ru/Mn/Ni(5:15:80) Al_2O_3	9.00	17.30	22.70	32.50

the catalyst and thus lead to decrease active sites on the surface of Ru catalyst. A similar finding was concluded by Nurunnabi et al. (2008). The residual chloride ions formed partition between the support and metal and thus, inhibits both CO and hydrogen chemisorption phenomena on the catalyst surface. Chloride precursor can be observed in the as-synthesis of Ru/Mn/Ni(5:35:60)/Al_2O_3 catalyst as shown in EDX data (Table 5).

When nickel loading was increased up to 80 wt%, the performance of the catalyst also increased with the increasing temperature reaction. The addition of palladium into this catalyst which is Pd/Mn/Ni(5:15:80)/Al_2O_3, coincidentally enhanced the catalytic activity of CO_2 conversion. Only 5.20% of CO_2 conversion at 100 °C reaction temperature increased to 49.00% at 400 °C reaction temperature. This suggests that a small amount of Pd can play important role in enhancing the catalytic activity. A study by Baylet et al. (2008) found that addition of palladium to the alumina support material gives sufficient absorption for CO_2 dissociation process which is due to the increasing active sites on catalyst surface. As expected, the addition of ruthenium into the catalyst also would increase the catalytic performance but slightly lower than the addition of palladium. Only 32.50% of CO_2 conversion was achieved at maximum studied temperature of 400 °C.

3.1.2. Catalytic activity screening of alumina supported nickel oxide based catalysts calcined at 700 °C for 5 h

The potential catalysts were further studied at 700 °C calcination temperature and the results are summarized in Table 2. At this stage, Ni(100)/Al_2O_3 catalyst displayed a slight increase in activity compare to the similar catalyst calcined at 400 °C. The addition of manganese into the system (Mn/Ni/Al_2O_3 catalyst), only 20% of CO_2 had been converted.

It can be observed that Pd/Mn/Ni(5:15:80)/Al_2O_3 shows the highest catalytic activity at the maximum reaction temperature of 400 °C. However, Pd/Mn/Ni(5:35:60)/Al_2O_3 showed lower activity (24.40%) compared to the other catalyst (Pd/Mn/Ni(5:15:80)/Al_2O_3). When ruthenium was used as co-dopant in Ru/Mn/Ni(5:35:60)/Al_2O_3 catalyst, it presented an

Table 2 Percentage CO_2 conversion over alumina supported nickel oxide based catalysts calcined at 700 °C for 5 h.

Catalysts	Reaction temperature (°C)			
	100	200	300	400
	% CO_2 conversion			
Monometallic oxide				
Ni(100)/Al_2O_3	2.70	3.42	9.43	15.60
Bimetallic oxide				
Mn/Ni(40:60)/Al_2O_3	2.10	3.40	7.40	18.30
Mn/Ni(20:80)/Al_2O_3	2.90	3.70	8.42	20.34
Trimetallic oxide				
Pd/Mn/Ni(5:35:60)/Al_2O_3	4.90	12.20	21.20	24.40
Ru/Mn/Ni(5:35:60)/Al_2O_3	1.60	4.30	10.50	34.00
Pd/Mn/Ni(5:15:80)/Al_2O_3	7.00	11.00	20.00	36.00
Ru/Mn/Ni(5:15:80)/Al_2O_3	1.20	4.70	8.90	13.60

increase of catalytic performance from 14.00% to 34.00% of CO_2 conversion when calcined at 400 °C and 700 °C, respectively. In contrast, at similar reaction temperature studied, the performance of Ru/Mn/Ni(5:15:80)/Al_2O_3 catalyst was slightly decreased from 32.50% at calcination temperature of 400 °C to 13.60% at calcination temperature of 700 °C.

This finding was supported by Murata and co-workers (2009) who studied the effect of Ru and Mn concentration on the Fischer–Tropsch reaction. They claimed that by increasing/decreasing Ru or Mn content it will affect the CO_2 conversion. The results showed that the CO_2 conversion and selectivity towards CH_4 were 42.9% and 9.10%, respectively using Ru to Mn ratio of 5:10. They also stated that the high CO_2 conversion was probably due to the Mn species which causes the removal of Cl ions from $RuCl_3$ precursor and increases the density of active Ru oxide species on the catalyst which resulted in a high catalytic activity. In contrast, Ru/Mn/Ni(5:15:80)/Al_2O_3 catalyst showed a low catalytic performance. It might be due to the calcination temperature applied on this catalyst cannot prevent the coke deposition onto the active site of the catalyst. Branford and Vannice (1998), suggested that reduction temperature more than 1000 °C is necessary to remove most residual Cl from supported catalysts.

3.1.3. Catalytic activity screening of alumina supported nickel based catalysts calcined at 1000 °C for 5 h

Table 3 exhibits the variation of catalytic performance over alumina supported nickel oxide based catalysts which were calcined at 1000 °C. Monometallic and bimetallic oxide catalysts exhibit a similar trend with increasing calcination temperature.

The addition of noble metals resulted in decreasing catalytic activity in both Pd/Mn/Ni(5:35:60)/Al_2O_3 and Pd/Mn/Ni(5:15:80)/Al_2O_3 catalysts. Further reduction might be because of Mn and Pd was not good oxide combination in methanation process and it will retard the process. This is in agreement with Panagiotopoulou et al. (2008) who found that Pd was found to be the least active catalyst which only gave less than 5% CO_2 conversion at 450 °C. The atomic size of Pd (137 pm) is much higher than that of Mn (127 pm). This may cause pore blockage because of the bigger size of Pd which retarded the methanation reaction.

Surprisingly, Ru/Mn/Ni(5:35:60)/Al_2O_3 catalyst showed the highest catalytic activity among the catalysts. The catalytic performance of this catalyst keeps on increasing until it reaches the maximum reaction temperature studied (400 °C). At the reaction temperature of 100 °C, only 7.50% CO_2 was converted but the performance turns to increase drastically until it reached 300 °C of reaction temperature. About 99.30% of CO_2 conversion was observed. At the maximum reaction temperature studied (400 °C), the catalytic activity was increased to 99.70% of CO_2 conversion. A similar catalytic behaviour has been observed on the other ratio of Ru/Mn/Ni(5:15:80)/Al_2O_3 catalyst calcined at 1000 °C, whereby the conversion is continuously increasing compared to the performance of similar catalyst calcined at 700 °C.

A research done by Samparthar et al. (2006) claimed that the total pore volume of the calcined samples will decrease as the loading of the transition metal oxides increases. The decreasing behaviour of both surface area and total pore volume with the increasing loading of metal oxides is consistent due to possible blockage of the inner pores especially the smaller ones. However, this finding cannot be proved in our research due to insufficient data. Similar reason can be applied to the Pd/Mn/Ni(5:15:80)/Al_2O_3 catalyst which displays a decreasing trend with the addition of nickel loading.

The above results suggested that the high calcination temperature activates the catalytic centres of the catalyst, thus enhancing the activity. The calcination temperatures are critical for controlling the size of the metal particles and their interaction with Al_2O_3 as suggested by Chen et al. (2009) who investigated the effect of calcination temperatures on nickel catalyst for methane decomposition. It was found that when the calcination temperature increases, the average size of the crystallites increases and it will help to increase the catalytic activity towards CO_2 conversion. In conclusion, Ru/Mn/Ni(5:35:60)/Al_2O_3 catalyst was selected as potential catalysts and was further investigated to seek the optimum condition for this catalyst.

3.2. Optimization of potential catalyst

Using Tables 1–3 as references, Ru/Mn/Ni(5:35:60)/Al_2O_3 catalyst calcined at 1000 °C was found to be the potential catalyst

Table 3 Percentage CO_2 conversion over alumina supported nickel oxide based catalysts calcined at 1000 °C for 5 h.

Catalysts	Reaction temperature (°C)			
	100	200	300	400
	% CO_2 conversion			
Monometallic oxide				
Ni(100)/Al_2O_3	8.24	10.10	12.63	17.80
Bimetallic oxide				
Mn/Ni(40:60)/Al_2O_3	9.30	13.80	17.24	20.10
Mn/Ni(20:80)/Al_2O_3	11.60	15.70	19.40	21.30
Trimetallic oxide				
Pd/Mn/Ni(5:35:60)/Al_2O_3	5.00	4.80	12.00	21.00
Ru/Mn/Ni(5:35:60)/Al_2O_3	7.50	25.00	99.30	99.70
Pd/Mn/Ni(5:15:80)/Al_2O_3	6.00	7.60	9.30	13.00
Ru/Mn/Ni(5:15:80)/Al_2O_3	9.10	13.60	21.50	51.00

Table 4 The product and by product of CO_2/H_2 methanation over $Ru/Mn/Ni(5:35:60)/Al_2O_3$ catalyst calcined at 1000 °C for 5 h detected by GC.

Catalysts	Reaction temperature (°C)	CO_2 conversion (%)		Unreacted CO_2 (%)*
		Product CH_4	By-product CO + H_2O	
$Ru/Mn/Ni(5:35:60)/Al_2O_3$				
	100	0.00	5.88	94.12
	200	15.26	5.04	79.70
	300	29.52	69.45	0.31
	400	72.36	27.38	0.26

* Unreacted CO_2 gas was calculated using FTIR analysis.

for CO_2/H_2 methanation reaction. Several optimization parameters were conducted on this catalyst including the effect of various compositions of catalyst, various calcination temperatures, effect of H_2S gas, reproducibility and stability testing.

3.2.1. Effect of various compositions of prepared catalyst

In order to determine the effect of various compositions towards the catalytic activity, 55–70 wt% of nickel loadings have been used in this research. The detailed trend plot of catalytic performance over $Ru/Mn/Ni(5:35:60)/Al_2O_3$ catalyst towards the percentage CO_2 conversion is displayed in Fig. 2. Generally, all the catalysts prepared showed lower performance of CO_2 conversion at low reaction temperature but started to increase drastically from 200 °C until maximum studied reaction temperature of 400 °C.

It can be seen that $Ru/Mn/Ni(5:40:55)/Al_2O_3$ catalyst only gave 15.54% CO_2 conversion at 200 °C reaction temperature. By raising the nickel content to 60 wt%, the conversion of CO_2 increased to 25.00%. However, the catalytic performance was reduced to 18.33% with the increasing of Ni loading to 70 wt% in the $Ru/Mn/Ni(5:25:70)/Al_2O_3$ catalyst. Mostly, these catalysts achieved more than 99% of CO_2 conversion at 300 °C reaction temperature. Catalyst labelled as $Ru/Mn/Ni/Al_2O_3$ with the ratio of 5:35:60 had been preferred to be the optimum ratio as it showed better performance at low reaction temperature.

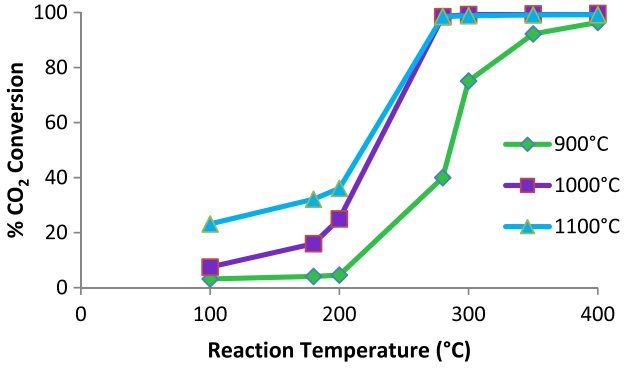

Figure 3 Catalytic performance of CO_2 conversion for CO_2/H_2 methanation reaction over $Ru/Mn/Ni(5:35:60)/Al_2O_3$ catalysts calcined at various calcination temperatures for 5 h.

From the catalytic performance, it can be concluded that the composition of the catalyst might cause the alteration of catalyst structure which is highly related to the catalytic performance and selectivity towards methanation reaction. Due to the high capability of $Ru/Mn/Ni(5:35:60)/Al_2O_3$ catalyst which contributed to high performance, this catalyst was

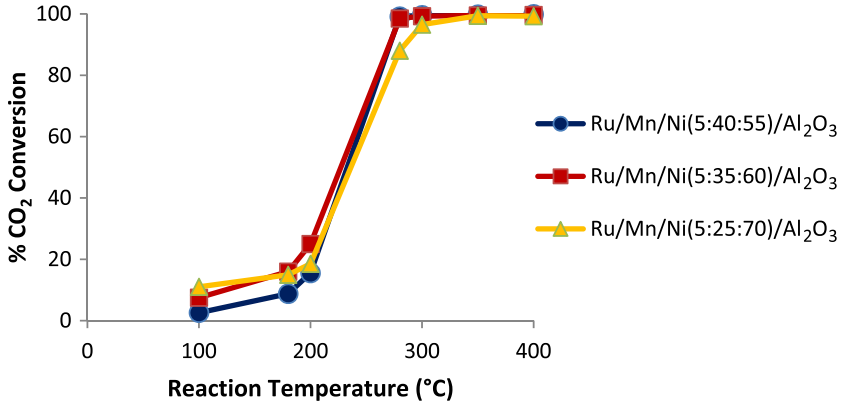

Figure 2 Catalytic performance of CO_2 conversion for CO_2/H_2 methanation reaction over $Ru/Mn/Ni/Al_2O_3$ catalyst at different compositions calcined at 1000 °C for 5 h.

further studied on the next parameter; the effect of various calcination temperatures.

3.2.2. Effect of different calcination temperatures

This parameter was conducted to determine the effect of various calcination temperatures on the most potential catalysts. Ru/Mn/Ni(5:35:60)/Al_2O_3 catalyst was prepared and coated on alumina support and then aged for 24 h before further calcined at three different temperatures of 900, 1000 and 1100 °C. Fig. 3 indicates the trend plot of catalytic activity over Ru/Mn/Ni(5:35:60)/Al_2O_3 catalyst at various calcination temperatures.

All the catalysts show increasing catalytic activity with the rise of reaction temperature. It has been revealed that the highest CO_2 conversion was obtained by Ru/Mn/Ni(5:35:60)/Al_2O_3 catalyst which was calcined at 1000 °C. From 25.00% of CO_2 conversion at 200 °C reaction temperature, it increased drastically to 99.70% conversion at the maximum reaction temperature studied (400 °C). However, the percentage of CO_2 conversion was slightly decreased to 99.20% at 400 when the catalyst was calcined at 1100 °C. Meanwhile, at 900 °C calcination temperature, about 96.40% of CO_2 conversion can be obtained at similar reaction temperature.

The high temperature used during calcination could cause agglomeration of catalyst particles thus forming larger crystallite and decreasing the surface area, consequently producing less active catalyst. According to Oh et al. (2007) the growth of crystallite size and morphology of the catalyst surface have strong relationship with calcination temperatures. This was in a good agreement with XRD diffractogram and FESEM morphology as will be discussed in characterization section after this.

Thus, it can be concluded that 1000 °C was the optimum calcination temperature over Ru/Mn/Ni(5:35:60)/Al_2O_3 catalyst. Both catalysts were then tested in the presence of H_2S gas in the gas mixtures.

3.2.3. Effect of H_2S gas over Ru/Mn/Ni(5:35:60)/Al_2O_3 catalyst

Durability testing of catalyst is an important factor for the practical use of catalysts. Hence, this test was carried out in the H_2/CO_2 gas mixture with a small amount of poison gas (H_2S), which commonly leads to deactivation of the catalyst. In this experiment, the respective catalyst was fed by 1% of

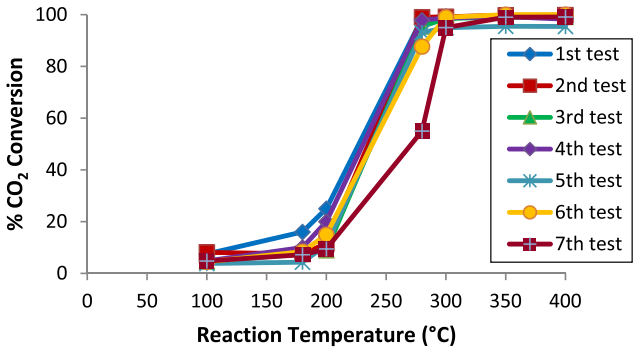

Figure 5 Trend plot of reproducibility testing over Ru/Mn/Ni(5:35:60)/Al_2O_3 catalyst calcined at 1000 °C for 5 h toward CO_2 conversion from methanation reaction.

H_2S gas during catalytic reaction. Fig. 4 indicates the comparison of catalytic activity with or without the presence of H_2S gas over Ru/Mn/Ni(5:35:60)/Al_2O_3 catalyst.

The Ru/Mn/Ni(5:35:60)/Al_2O_3 catalyst was not able to achieve 100% H_2S desulfurization as shown in Fig. 4. It can only convert 41% of H_2S to elemental sulfur at 100 °C reaction temperature and increased up to 86% at the 300 °C reaction temperature studied. After 300 °C reaction temperature, the catalyst started to deactivate due to the sulfur deposition on the catalyst surface. Consequently, the CO_2 conversion over Ru/Mn/Ni(5:35:60)/Al_2O_3 catalyst decreased significantly in the presence of hydrogen sulfide gas mixtures from 99.70% (without H_2S) to 7.5% (with H_2S).

The deterioration of the catalyst occurred at higher reaction temperature owing to sulfur formation which had covered the surface catalyst thus avoiding the next flowing H_2S to be converted hence retard the reduction of CO_2 during methanation reaction (Wan Abu Bakar et al., 2011). Moreover, a research done by Dokmaingam et al. (2007) also supports our finding because similar phenomenon occurred in their methane steam reforming reaction in which their activity rate dramatically decreased over Ni/Al_2O_3 and Ni/CeO_2 in the presence of H_2S due to the sulfidation on the surface of the catalysts.

Unexpectedly, carbon monoxide has been observed in FTIR spectrum during reaction in the presence of H_2S gas. It is probably because of incomplete reaction between CO_2 and H_2 which tends to form CO as intermediate species (not

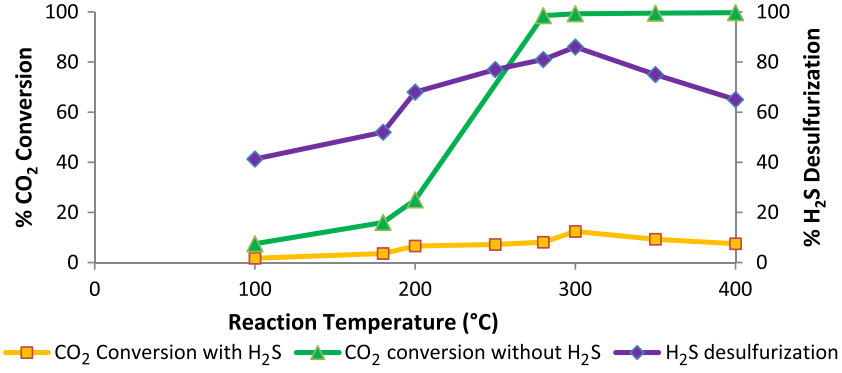

Figure 4 Effect of the presence of H_2S gas over Ru/Mn/Ni(5:35:60)/Al_2O_3 catalyst calcined at 1000 °C for 5 h.

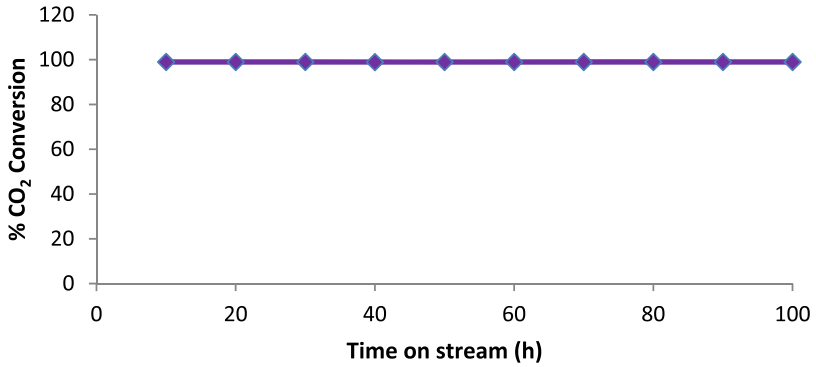

Figure 6 Stability test over Ru/Mn/Ni(5:35:60)/Al_2O_3 catalyst calcined at 1000 °C for 5 h at 250 °C reaction temperature.

shown). No methane peak can be distinguished. The toxic H_2S gas will prevent the catalyst to convert reactant gases; CO_2 and H_2 to produce methane.

3.2.4. Reproducibility test towards potential catalyst

The reproducibility of catalytic activity over Ru/Mn/Ni(5:35:60)/Al_2O_3 catalyst was tested using the similar potential catalyst for several times until the catalyst deactivated. Fig. 5 shows the trend plot of reproducibility testing over Ru/Mn/Ni(5:35:60)/Al_2O_3 catalyst.

Below 200 °C of reaction temperature, it can be seen that the percentage CO_2 conversion was slightly lower than 26.00%. Interestingly, increasing the temperature above 200 °C, a sharp inclination occurred and achieved 99% CO_2 conversion at 280 °C reaction temperature and continuously to do so until it reached the maximum reaction temperature studied (400 °C). It can be distinguished that from 1st test until 7th test, the catalytic performance was almost similar. However, after the seventh testing, catalytic activity slightly decreased to 55% CO_2 conversion at 280 °C reaction temperature but still active at high reaction temperature. It is probably due to the surface of catalyst which was covered by CO_2 thus slightly decreasing the catalytic performance.

3.2.5. Stability testing over the Ru/Mn/Ni(5:35:60)/Al_2O_3 catalyst

The catalytic stability of the potential Ru/Mn/Ni(5:35:60)/Al_2O_3 catalyst was investigated on stream for 5 h continuously at 250 °C reaction temperature as presented in Fig. 6. The Ru/Mn/Ni(5:35:60)/Al_2O_3 catalysts showed a good stability which was maintained unaffected for 5 h of maximum monitoring reaction time without deterioration by carbon. The CO_2 conversion of Ru/Mn/Ni(5:35:60)/Al_2O_3 catalyst was maintained at almost 100% throughout the reaction time.

Even though nickel oxide catalyst is easily deactivated by carbon deposition, the addition of manganese and ruthenium would assist the catalyst to be stable during the reaction. This was in good agreement with Zhao et al. (2012) who found that modifying nickel based with manganese significantly leads to the most stable catalyst compared to the unmodified NiO/Al_2O_3 catalyst. From these results, it can be concluded that the Ru/Mn/Ni(5:35:60)/Al_2O_3 catalyst is still active and stable even if it was left on for 5 h under high reaction temperature.

3.2.6. Methane gas formation measurement via gas chromatography

The reactor gas product from FTIR cell was collected and analyzed for CH_4 formation. The methane formation was

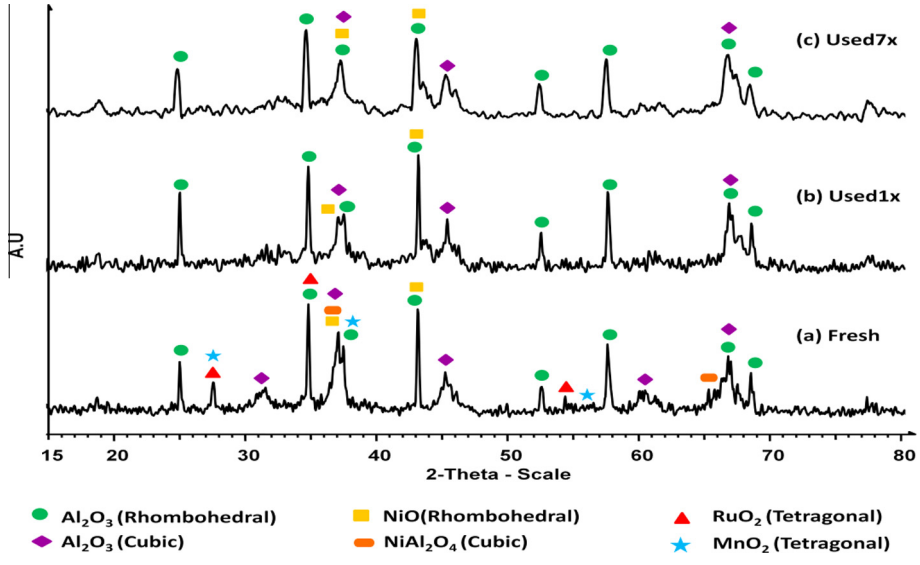

Figure 7 XRD patterns of Ru/Mn/Ni(5:35:60)/Al_2O_3catalysts calcined at 1000 °C for 5 h.

determined via GC because of low sensitivity of FTIR spectroscopy towards methane stretching region. Table 4 shows the catalytic activity of CO_2/H_2 methanation over the potential $Ru/Mn/Ni(5:35:60)/Al_2O_3$ catalyst.

There are three possible products obtained during CO_2/H_2 methanation reaction namely carbon monoxide, water and methane. A trend could be noticed that the percentage of unreacted CO_2 decreased as the CO_2 was converted to H_2O, CO and CH_4. Besides, the formation of CH_4 also increased as reaction temperature increased. In the $Ru/Mn/Ni(5:35:60)/Al_2O_3$ catalyst, none of methane production has been observed at 100 °C reaction temperature but converted CO_2 tends to yield by- products such as CO and H_2O. The higher methane formation was reached at 400 °C with 72.36%.

These results are in a good agreement with Yaccato et al. (2005) who found that at lower temperature, methanation reaction tends to yield CO and at higher reaction temperature CH_4 was formed. The higher methane formation was reached at 250 °C with 76%. Higher methane has been produced possibly attributed to the rapid hydrogenation of intermediate CO species resulting in higher CO_2 methanation activities at this temperature.

3.3. Characterization of potential catalyst on methanation reaction

3.3.1. The effect of catalytic testing over Ru/Mn/Ni(5:35:60)/Al_2O_3 catalyst calcined at 1000 °C for 5 h by XRD analysis

Fig. 7 shows the XRD patterns for potential $Ru/Mn/Ni(5:35:60)/Al_2O_3$ catalyst which was calcined at 1000 °C for 5 h. XRD diffractograms for used catalysts were found to be similar with fresh catalyst in which owing polycrystalline with some amorphous phase in nature.

The XRD pattern over $Ru/Mn/Ni(5:35:60)/Al_2O_3$ catalyst calcined at 1000 °C in fresh condition showed the presence of several oxides on the surface catalyst. High crystallinity of rhombohedral Al_2O_3 can be observed at 2θ of 35.10 (I_{100}), 43.34 (I_{94}), 57.48 (I_{79}), 25.56 (I_{74}), 37.70 (I_{45}), 52.50 (I_{42}), 68.17 (I_{41}) and 66.37° (I_{28}) with d values of 2.55, 2.08, 1.60, 3.47, 2.38, 1.74, 1.37 and 1.40 Å (PDF d values of 2.55, 2.08, 1.60, 3.48, 2.38, 1.74, 1.37 and 1.40 Å). However, there is some amorphous character within the crystalline peak which belongs to the alumina cubic indicating the smaller particle sizes owing to the respective catalyst. Interestingly, new peaks attributable to the NiO rhombohedral phase species were observed at 2θ of 43.40 (I_{98}) and 37.38 (I_{95}) with d values of 2.08 and 2.40 Å (PDF d values of 2.08 and 2.41 Å). Meanwhile, RuO_2 tetragonal species intensely located at 2θ of 35.19 (I_{100}), 28.10 (I_{32}) and 54.44 (I_{19}) with d values of 2.55, 3.17 and 1.68 Å (PDF d values of 2.55, 3.17 and 1.68 Å)were observed. However, the intensity for MnO_2 tetragonal was very small and hardly distinguished from the background noise. It is probably because of MnO_2 present in low quantities and overlapped with other species thus less sensitive towards XRD analysis. Unexpectedly, two peaks assigned as $NiAl_2O_4$ species have been detected at 2θ of 37.38 (I_{100}) and 65.64°(I_{43}) with d values of 2.40 and 1.42 Å (PDF d values of 2.42 and 1.42 Å) but not obviously can be seen.

It is noteworthy that Al_2O_3 still remains in rhombohedral and cubic phases after catalytic testing (Fig. 7(b)). Meanwhile, NiO species were observed in rhombohedral phase which present in lower intensity. Unexpectedly, $NiAl_2O_4$, RuO_2 and MnO_2 species were disappeared in both used $Ru/Mn/Ni(5:35:60)/Al_2O_3$ catalysts suggesting the well dispersion of these species on the surface of the catalysts that below the

Table 5 EDX analysis of fresh and used catalysts $Ru/Mn/Ni(5:35:60)/Al_2O_3$ calcined at 1000 °C.

Catalyst	Weight ratio (%)					
	Al	O	Ni	Mn	Ru	Cl
As-synthesis	49.04	37.61	6.16	2.49	1.43	3.29
Fresh	56.42	29.36	5.79	4.35	4.08	–
Used1x	56.14	39.31	3.06	0.43	1.06	–
Used7x	55.42	39.23	4.51	0.27	0.58	–

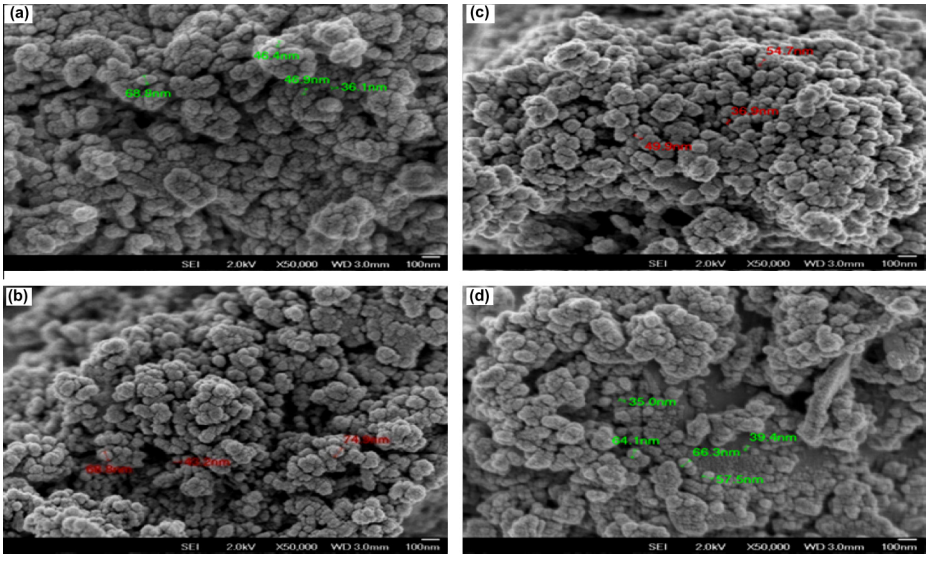

Figure 8 FESEM micrographs of $Ru/Mn/Ni(5:35:60)/Al_2O_3$ calcined at 1000 °C for 5 h, (a) as-synthesis, (b) fresh, (c) used1x, (d) used7x.

XRD detection limit. Wan Abu Bakar et al. (2010) revealed that some species collapse after undergoing catalytic testing due to the well dispersion of these particles into the bulk matrix of the catalyst. This phenomenon also can be supported by Zhao et al. (2012) who found no manganese oxide crystalline phase can be detected by XRD analysis after catalytic testing.

The continuous emergence of NiO in Ru/Mn/Ni(5:35:60)/Al_2O_3 catalyst (before and after catalytic testing) may suggested that this species can be considered as active species. The recommended active species had increased the percentage removal of CO_2 and at the same time increase the formation of CH_4 as had been discussed before.

3.3.2. The effect of catalytic testing by FESEM-EDX analysis on Ru/Mn/Ni(5:35:60)/Al_2O_3 catalyst calcined at 1000 °C for 5 h

Fig. 8 shows the effect of catalytic testing on the Ru/Mn/Ni(5:35:60)/Al_2O_3 catalysts in various conditions for instance as synthesis (before calcine), fresh (before reaction), used1x and used7x (after reaction) catalysts.

Table 6 BET surface area and pore diameter of fresh and used catalysts Ru/Mn/Ni (5:35:60)/Al_2O_3 calcined at 1000 °C.

Catalyst	Condition	S_{BET} (m^2/g)	Average pore diameter (Å)	Isotherm plot
Ru/Mn/Ni(5:35:60)/Al_2O_3	Alumina	192	–	–
	Fresh	47	140	Type IV
	Used1x	60	88	Type IV
	Used7x	56	94	Type IV

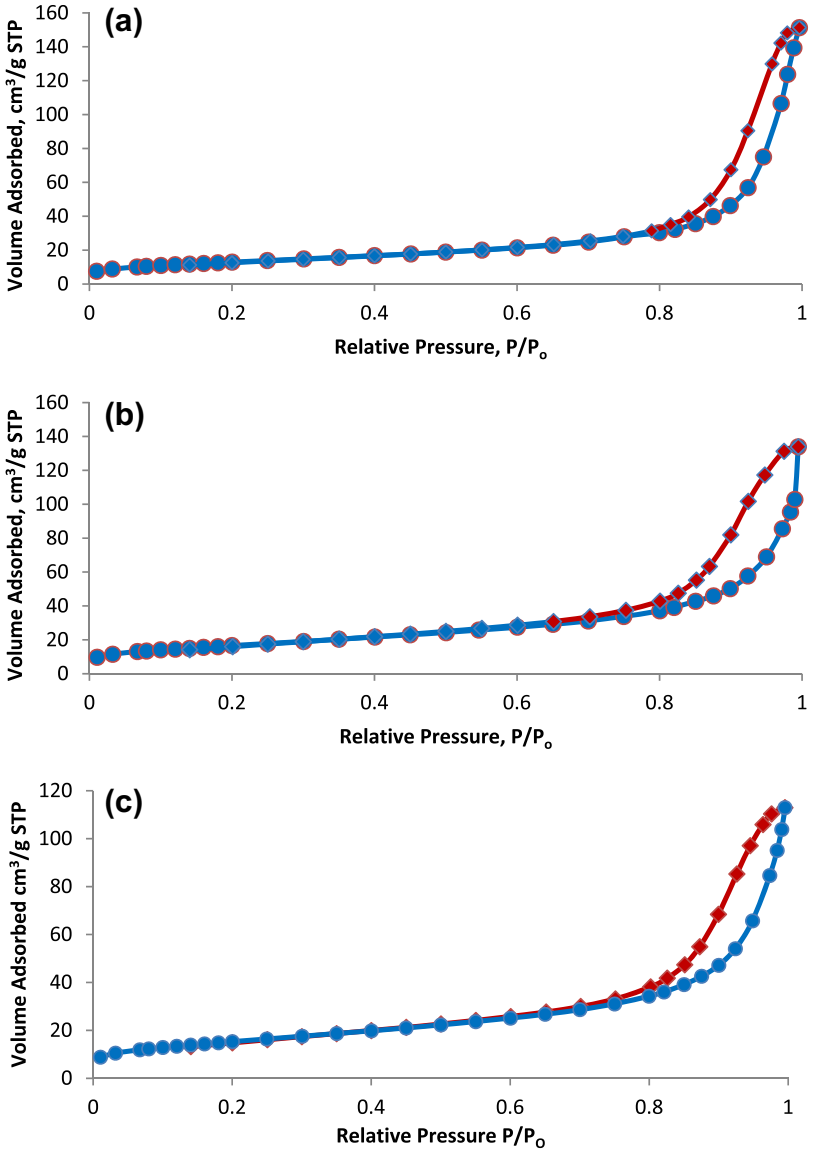

Figure 9 Isotherm plots of Ru/Mn/Ni (5:35:60)/Al_2O_3 calcined at 1000 °C, fresh, (b) used1x, (c) used7x.

These catalysts display inhomogeneous mixtures of aggregated and agglomerated particles in spherical shape. Additionally, these catalysts have been proved to be nano categorised since their particle sizes are in the range of 36–75 nm. Furthermore, these findings were well supported by XRD diffractograms denoted as polycrystalline with some amorphous character for all catalysts (Fig. 7). Smaller particles size lead to higher metal dispersion and thus increase the surface area of the catalyst as well as catalytic activity. From the micrographs, it also can be noted that the average particle size of as-synthesis, fresh and used catalysts remained unchanged suggesting that no significant changes occurred under reaction conditions.

Meanwhile, EDX analysis for all Ru/Mn/Ni(5:35:60)/Al_2O_3 catalysts confirmed the presence of Al, O, Ni, Mn and Ru. As written in Table 5, the percentage of weight ratios for each element in used catalyst was decreased compare to the fresh catalyst except for oxygen atom (O). Al and O contributed the highest percentage of weight ratio since the usage of alumina (Al_2O_3) as support in this research. As-synthesis catalyst showed the presence of 6.16 wt% of Ni, 2.49 wt% of Mn, and 1.43 wt% of Ru as well 3.29 wt% of chloride precursor has been detected.

The fresh Ru/Mn/Ni (5:35:60)/Al_2O_3 catalyst had attained 5.79 wt% of Ni, 4.35 wt% of Mn and 4.08 wt% of Ru. After catalytic testing, the weight ratio of each element became lower. After seventh testing, a small amount of 0.58 wt% and 0.27 wt% of Ru and Mn, respectively, can be detected compared to Ni element. These results are supported by XRD analysis (Fig. 7) in which only NiO in rhombohedral phase is profoundly observed. In contrast, MnO_2 and RuO_2 peaks are hard to distinguish from noise background probably due to the lesser amount of these species as detected by EDX (Table 5).

The reduction in weight ratio of Ni, Mn and Ru of used catalyst is probably due to the well dispersion of these particles onto the support. This phenomenon might explain the migration of Ni, Mn and Ru into the bulk matrix of the catalyst surface resulting in lesser particles that can be detected by EDX analysis on the surface of the catalyst. Besides, this result was in a good agreement with Nurunnabi et al. (2008), who said that the Ru may have been adsorbed into the porous support consequently lowering the concentration of Ru on the surface. Meanwhile, no Cl element was observed in fresh and used catalysts indicating that calcination completely removes chloride precursor.

3.3.3. The effect of catalytic testing on Ru/Mn/Ni(5:35:60)/Al_2O_3 catalyst calcined at 1000 °C for 5 h by nitrogen adsorption analysis

The BET surface area and average pore diameter for the potential Ru/Mn/Ni(5:35:60)/Al_2O_3 catalyst are listed in Table 6. According to Zhao et al. (2012), surface area for neat alumina support which mainly contributed by the micro/meso-pores and capillary effect plays the dominating role during impregnation. Thus, Al_2O_3 pores offer a space for the access of active Ni and Mn elements.

In this research, alumina has 192 m^2/g of surface area. After impregnation process, some alumina pores will be blocked which may contribute to the decreasing surface area and pore diameter of the catalysts. From Table 6, it can be seen that surface area of fresh Ru/Mn/Ni(5:35:60)/Al_2O_3 catalyst is smaller about 47 m^2/g with 140 Å pore diameter compared to the neat alumina support.

After catalytic testing, the surface area of the catalyst increased to 60 m^2/g. This increment is probably due to the smaller particle size contributing to the higher surface area. However, after seventh testing, the surface area of used catalyst was slightly decreased compare to the used1x catalyst. A trend could be observed that by increasing the surface area, the average pore diameter decreases. As a result, average pore diameter became smaller after catalytic testing indicating that some pores are blocked by the larger crystallite.

The nitrogen adsorption–desorption isotherms for both fresh and used of Ru/Mn/Ni(5:35:60)/Al_2O_3 catalysts are

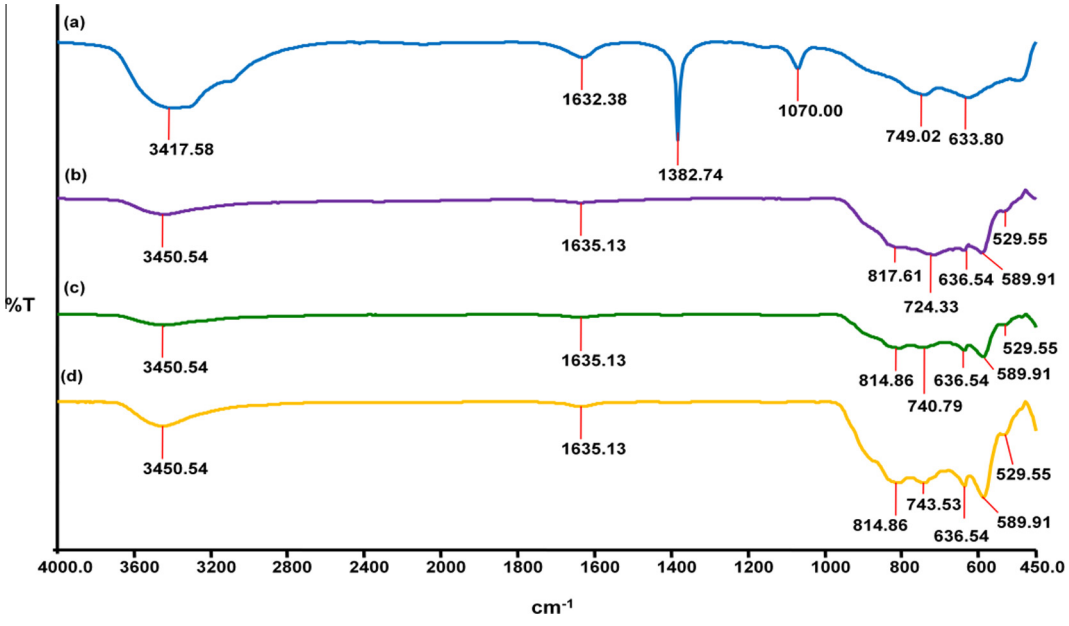

Figure 10 FTIR spectra of Ru/Mn/Ni (5:35:60)/Al_2O_3 calcined at 1000 °C, (a) as-synthesis, (b) fresh, (c) used1x, (d) used7x.

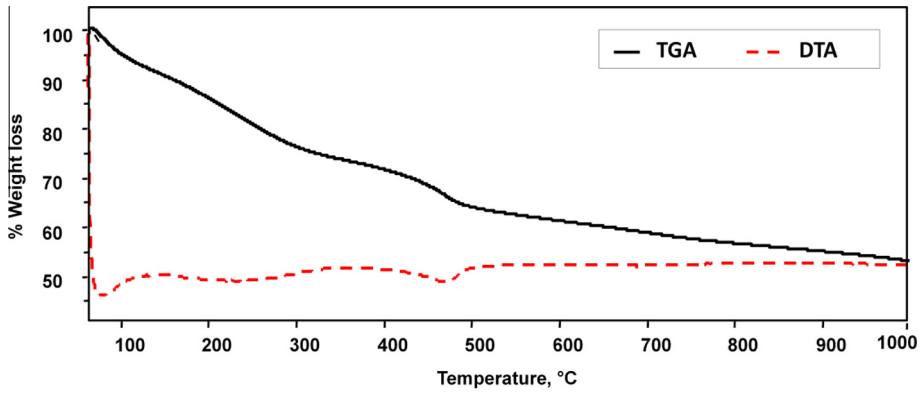

Figure 11 TGA-DTA thermogram of as-synthesis Ru/Mn/Ni(5:35:60)/Al_2O_3 catalyst.

shown in Fig. 9. This catalyst exhibits isotherm Type IV with hysteresis loop of type H1 indicating that the catalysts were in mesoporous structure (20 Å < W < 500 Å). Moreover, hysteresis loop of type H1 assigned that the catalysts are in open ended cylindrical channel with uniform shape and size as indicated in FESEM analysis.

3.3.4. Fourier Transform Infra-Red (FTIR) analysis on Ru/Mn/Ni(5:35:60)/Al_2O_3 catalyst calcined at 1000 °C for 5 h

Fig. 10 displays the FTIR spectra of as-synthesis, fresh and used Ru/Mn/Ni(5:35:60)/Al_2O_3 catalysts calcined at 1000 °C for comparison.

It can be observed that the FTIR spectra for these catalysts in different conditions remained similar suggesting similar functional groups present in these catalysts. The presence of the OH group from adsorbed water molecule is revealed by absorption peaks at 3390–3445 cm^{-1} and 1631–1635 cm^{-1}, respectively as OH stretching and bending modes of vibration. These peaks diminished after calcination process. However, the O–H band emerged after seventh testing from water as by-product in the methanation reaction.

The absorption below 1071 cm^{-1} was assigned as the stretching mode of metal oxide (M═O) groups which indicated that the oxide catalysts have been obtained as all impurities have been removed. Meanwhile, some nitrate precursor residues were left in the catalyst due to the strong absorption peak at 1384 cm^{-1} for the as-synthesis catalyst (Fig. 10(a)). However, nitrate precursor has been removed through calcination process as proven in the fresh and used catalysts. It is believed that nitrate precursor has been completely removed at 1000 °C calcination temperature.

3.3.5. Thermogravimetry Analysis–Differential Thermal Analysis (TGA-DTA) on Ru/Mn/Ni(5:35:60)/Al_2O_3 catalyst

The potential Ru/Mn/Ni(5:35:60)/Al_2O_3 catalyst in as-synthesis condition which was produced by impregnation method and after aged overnight in oven at 80–90 °C was characterized by TGA–DTA analysis in order to study thermal activity as shown in Fig. 11.

Overall, total weight loss that was observed in this sample is 19.66%. At the starting point of temperature studied (60 °C) until 120 °C, there was 2.79% of weight loss which equalled to 0.1325 mg, assigned to the loss of surface free water molecule. On the other hand from 120 °C until 330 °C, the decomposition of surface hydroxyl molecule from the sample was observed. From 330 °C onwards, nitrate compound and surface hydroxyl molecule were decomposed. At 1000 °C, the impurities from the catalyst have been removed and pure metal oxide can be obtained.

DTA analysis supports the weight loss of sample from TGA analysis. A small endothermic peak can be seen below 100 °C which assigned to the dehydration process where the loss of surface water occurred. Then, a broad endothermic peak at 200 °C until 300 °C attributed to the surface hydroxyl was observed. A significant thermal difference can be detected at 450 °C which is due to loss of surface hydroxyl molecule and the decomposition of residual nitrate. This finding was supported by Wan Abu Bakar and co-workers, 2012.

It can be concluded that at 1000 °C calcination temperature is effective in removing all impurities as has been proven by FTIR, EDX and TGA-DTA analysis. Furthermore, a higher activity can be achieved at the optimum 1000 °C calcination temperature.

4. Conclusion

Overall performance from the catalytic activity studies did not produce any catalyst that can achieve 100% of CO_2 conversion at low reaction temperature. However, Ru/Mn/Ni(5:35:60)/Al_2O_3 calcined at 1000 °C was assigned as the potential catalyst because of the contribution of 99.74% of CO_2 conversion and 72.36% of CH_4 formation at the maximum reaction temperature studied (400 °C). From XRD analysis, this supported catalyst showed in polycrystalline with some amorphous phase suggesting NiO as active species which was supported by FESEM analysis. This catalyst is categorised as nanoparticle in spherical shape with aggregated and agglomerated mixtures on the surface of the catalyst. Moreover, this catalyst exhibits a small surface area of 47 m^2/g and possesses a mesoporous structure as shown by isotherm of Type IV. Calcination temperature of 1000 °C successfully removed the impurities as shown by FTIR, EDX and TGA–DTA data.

Acknowledgement

The authors would like to thank the Ministry of Higher Education for GUP fund vote 01H79 and University Teknologi Malaysia for financial support.

References

Azadi, P., Otomo, J., Hatama, H., Oshima, Y., Farnood, R., 2001. Interactions of supported nickel and nickel oxide catalysts with methanation and steam at high temperature. Chem. Eng. Sci. 66, 4196–4202.

Baylet, A., Royer, S., Marecot, P., Tatibouet, J.M., Duprez, D., 2008. High catalytic activity and stability of Pd doped hexaaluminate catalysts for the CH_4 catalytic combustion. Appl. Catal. B 77, 237–247.

Branford, M.J.C., Vannice, M.A., 1998. CO_2 reforming of CH_4 over supported Ru catalysts. J. Catal. 183, 69–75.

Chen, J., Ma, Q., Rufford, T.E., Li, Y., Zhu, Z., 2009. Influence of calcination temperatures of Feitknecht compound precursor on the structure of Ni–Al_2O_3 catalyst and the corresponding catalytic activity in methane decomposition to hydrogen and carbon nanofibers. Appl. Catal. A 362, 1–7.

Dokmaingam, P., Palikanon, T., Laosiripojana, N., 2007. Effect of H_2S, CO_2, and O_2 on catalytic methane steam reforming over Ni/CeO_2 and Ni/Al_2O_3 catalysts. KMUTT Res. Dev. J. 30 (1), 36–47.

Mok, Y.S., Kang, H.C., Lee, H.J., Koh, D.J., Shin, D.N., 2010. Effect of nonthermal plasma on the methanation of carbon monoxide over nickel catalyst. Plasma Chem. Plasma Process. 30, 437–447.

Murata, K., Okabe, K., Inaba, M., Takahara, I., Liu, Y., 2009. Mn-modified Ru catalysts supported on carbon nanotubes for Fisher Tropsch synthesis. J. Jpn. Petrol. Inst. 52 (1), 16–20.

Nurunnabi, M., Muruta, K., Okabe, K., Inaba, M., Takahara, I., 2008. Performance and characterization of Ru/Al_2O_3 and Ru/SiO_2 Catalysts modified with Mn for Fisher-Tropsch synthesis. Appl. Catal., A 340, 203–211.

Oh, S.W., Bang, H.Y., Bae, Y.C., Sun, Y.K., 2007. Effect of calcinations temperature on morphology, crystallinity and electrochemical properties of nano-crystalline metal oxides (Co_3O_4, CuO and NiO) prepared via ultrasonic spray pyrolysis. J. Power Sources 173, 502–509.

Ouaguenouni, M.-H., Benadda, A., Kiennemann, A., Barama, A., 2009. Preparation and catalytic activity of nickel–manganese oxide catalysts in the reaction of partial oxidation of methane. C. R. Chim. 12, 740–747.

Panagiotopoulou, P., Kondarides, D.I., Verykios, X., 2008. Selective Methanation of CO over supported noble metal catalysts: effects of the nature of the metallic phase on catalytic performance. Appl. Catal., A 344, 45–54.

Park, J.H., Lee, D., Lee, H.C., Park, E.D., 2010. Steam reforming of liquid petroleum gas over Mn-promoted Ni/γ–Al_2O_3 catalysts. Korean J. Chem. Eng. 27 (4), 1132–1138.

Richardson, J.T., 1982. Principles of Catalyst Development. Plenum Press, Houston, Texas, New York and London.

Samparthar, J.T., Xiao, H., Dou, J., Nah, T.Y., Rong, X., Kwan, W.P., 2006. A novel oxidative desulfurization process to remove refractory sulfur compound from diesel fuel. Appl. Catal. B 63 (1–2), 85–93.

Wan Abu Bakar, W.A., Ali, R., Abdul Kadir, A.K., Mat Rosid, S.M., Ali, R., Mohammad, N.S., 2012. Catalytic methanation reaction over alumina supported cobalt oxide doped noble metal oxides for the purification of simulated natural gas. *J. Fuel Chem. Technol.* 40 (7), 822–830.

Wan Abu Bakar, W.A., Ali, R., Sulaiman, N., Abd Rahim, H.F., 2010. Manganese oxide doped noble metals supported catalyst for carbon dioxide methanation reaction. *Sci. Iranica* 17 (2), 115–123.

Wan Abu Bakar, W.A., Ali, R., Toemen, S., 2011. Catalytic methanation reaction over supported nickel–rhodium oxide for purification of simulated natural gas. J. Nat. Gas Chem. 20, 585–594.

Yaccato, K., Carhart, R., Hagemeyer, A., Lesik, A., Strasser, P., Volpe Jr., A.F., Turner, H., Weinberg, H., Grasselli, R.K., Brooks, C., 2005. Competitive CO and CO_2 Methanation over supported noble metal catalysts in high throughout scanning mass spectrometer. Appl. Catal. A 296, 30–48.

Zhao, A., Ying, W., Zhang, H., Ma, H., Fang, Dingye, 2012. Ni/Al_2O_3 catalysts for syngas methanation: effect of Mn promoter. J. Nat. Gas Chem. 2, 170–177.